Available online at www.sciencedirect.com
SCIENCE DIRECT®
Advances in Space Research 33 (2004) 1905–1912
ADVANCES IN SPACE RESEARCH (a COSPAR publication)
www.elsevier.com/locate/asr

Induced magnetospheres

J.G. Luhmann [a,*], S.A. Ledvina [a], C.T. Russell [b]

[a] Space Sciences Laboratory, University of California, Grizzly Peak Blvd., Centennial Drive, Berkeley, CA 94720, USA
[b] Institute of Geophysics and Planetary Physics, University of California, Los Angeles, CA 90095-1567, USA

Received 6 January 2003; received in revised form 21 March 2003; accepted 25 March 2003

Abstract

Induced magnetospheres occur around planetary bodies that are electrically conducting or have substantial ionospheres, and are exposed to a time-varying external magnetic field. They can also occur where a flowing plasma encounters a mass-loading region in which ions are added to the flow. In this introduction to the subject we examine induced magnetospheres of the former type. The solar wind interaction with Venus is used to illustrate the induced magnetosphere that results from the solar wind interaction with an ionosphere.
© 2004 COSPAR. Published by Elsevier Ltd. All rights reserved.

Keywords: Induced magnetospheres; Magnetic obstacle; Plasma interaction

1. Introduction

Most readers are familiar with the traditional picture of a magnetosphere, illustrated in Fig. 1(a). Its dipolar magnetic field from an internal planetary dynamo is distorted by the solar wind flow into a blunt obstacle shape, surrounded by a magnetosheath of shocked, deflected solar wind plasma with its draped, frozen-in magnetic field. It is defined as the region of space in which the magnetic field lines have at least one end connected to the source of the internal field. The magnetopause is the outer boundary of this topological domain. In contrast, an induced magnetosphere occurs in plasma interactions with nonmagnetic bodies, and is the less well-defined region in which magnetic forces dominate the dynamics of the plasma. The word "induced" in this context refers to the general process of creating an effective magnetic obstacle through the plasma interaction. The induced magnetic fields include the classical field perturbations resulting from electromagnetic induction, but also the field perturbations from the flow interaction. The obstacle producing the induced magnetosphere can be an electrically conducting, compressible ionospheric shell that balances the external plasma pressure at an ionopause, or an incompressible conducting body, such as an iron core or salt-water ocean, whose classically induced external field perturbation deflects the ambient flow and field around the obstacle. In this introduction to the subject, we first consider what makes an induced magnetosphere. An idealized MHD simulation of Venus in the solar wind is then used to illustrate the prototypical induced magnetosphere created by a planetary ionosphere, and to point out some of the complications and still unobserved aspects of these plasma interactions.

2. What is an induced magnetosphere?

Induced magnetospheres are found in the magnetized plasmas of the solar wind, as in the case of Venus (Russell and Vaisberg, 1983), or in planetary magnetospheres, as at Titan (Ness et al., 1982). Their existence depends on currents induced on or within a body or its ionosphere by temporal changes in direction and/or magnitude in the external magnetic field on time scales short compared to that for the field to diffuse into the conductor. If the conductor is an ionosphere, the obstacle and the resulting interaction is partially controlled by the dynamic pressure of the incident plasma. The

* Corresponding author. Tel.: +1-510-642-2545; fax: +1-510-643-8302.
E-mail address: jgluhmann@ssl.berkeley.edu (J.G. Luhmann).

0273-1177/$30 © 2004 COSPAR. Published by Elsevier Ltd. All rights reserved.
doi:10.1016/j.asr.2003.03.031

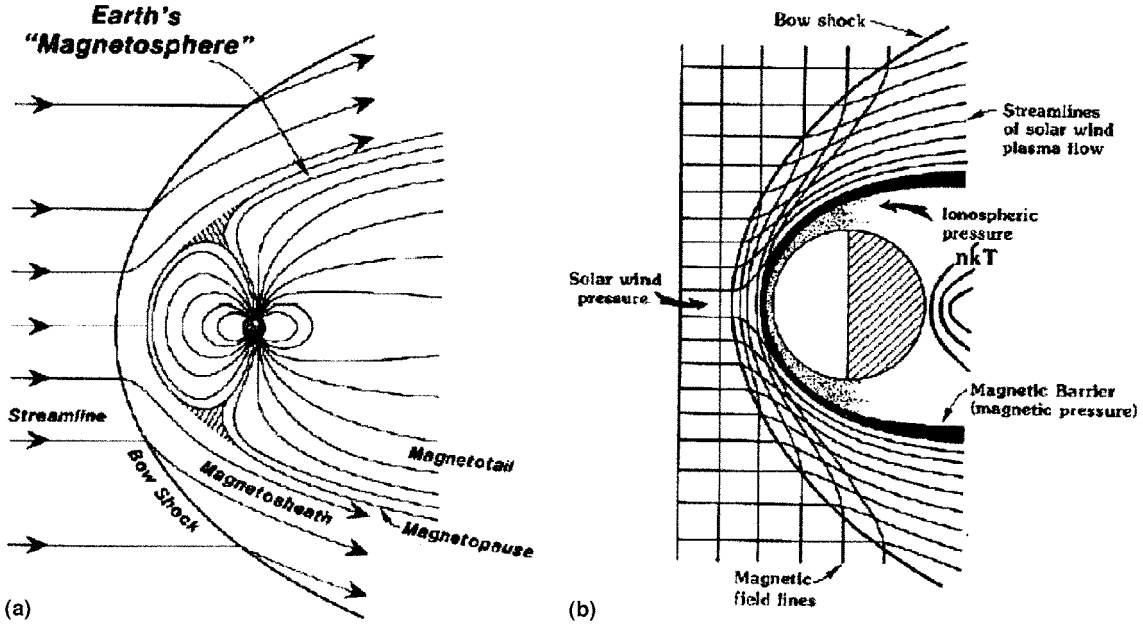

Fig. 1. Illustration of a traditional magnetosphere, like that of Earth (a), characterized by its region of planetary field-dominated space inside of a magnetopause outer boundary, and an induced magnetosphere (b), like that of Venus, where the ionospheric pressure forms the obstacle to the solar wind.

magnetic fields associated with the induced currents are generally configured so as to exclude the external field from the conductor. The disturbed field regions in fast flows include a magnetosheath and an induced magnetotail that is essentially an extension of the magnetosheath into the wake. Fig. 1(b) illustrates these features for an ionospheric obstacle, and the contrast to the traditional magnetosphere in Fig. 1(a).

The existence of a bow shock at the upstream boundary of an induced magnetosphere's magnetosheath depends on the combination of magnetosonic Mach number of the relative external flow, the importance of ion pickup from any extended atmosphere of the obstacle, and the importance of finite-ion gyroradius effects. In particular, mass loading by ion pickup from an extended atmosphere can gradually slow the external flow, making a shock flow transition unnecessary. Ion pickup can moreover dominate a plasma interaction to the extent that induced currents are unimportant compared to mass loading of the surrounding plasma by the pickup ions. Comets exhibit induced magnetotails in the solar wind, but they are primarily due to localized slowing of the solar wind in the space surrounding the nucleus by production of water and other heavy ions on passing interplanetary magnetic flux tubes. For this reason cometary interactions are placed in a separate category, to be discussed elsewhere in this volume by T.E. Cravens. The importance of the dynamic pressure of the cometary gas outflow in defining the cometary obstacle (Lindgren et al., 1997) also distinguishes comets from most planetary induced magnetospheres (with the possible exception of Pluto, see Bagenal et al., 1998). Similarly, for discussion of finite-ion gyroradius effects, which can prevent the formation of an MHD shock if the subflow magnetosheath thickness is comparable to or less than the ions' gyroradii, we refer the reader to a later paper by Ledvina et al. (also this volume).

The lifetime of the classical induction currents contributing to the induced magnetosphere depends on the electrical conductivity of the material involved and the dimensions of the body in which these currents are generated, together with the frequency of the external magnetic field changes. For planets or planetary satellites, these currents may flow in parts of the interior body and on the surface of conductors such as molten core material or liquid layers such as oceans. They can also flow in the ionosphere if an atmosphere is present, in a current layer or ionopause boundary layer where the external magnetized plasma and ionospheric plasmas balance. While we do not usually think of these currents as classically induced, the ionopause effectively acts as a conducting surface. The currents associated with pressure balance with a completely collisionless ionosphere can last indefinitely, as long as the pressure gradients at the boundary are maintained by the flowing external plasma and the ionosphere is maintained by solar EUV. If the ionosphere is resistive at the pressure balance altitude, the "shielding" current spreads as the magnetic field diffuses into the ionosphere. We note that if the solar wind interacted with an atmosphereless planet but the body of the planet was molten metal with a very high electrical conductivity, a shielding current would flow on the outer surface of the metal planet and a similar induced magnetosphere would be created.

It was once thought that the Earth's Moon would produce an induced magnetosphere in the solar wind. The dipolar field that would be classically induced in its conducting interior by interplanetary magnetic field variations is illustrated in Fig. 2(a) for the simplified case of an external vacuum field. In the fast-flowing plasma of the solar wind the magnetic configuration would be more like that shown in Fig. 2(b), with an upstream bow shock bounding the perturbed field. However, the early missions to the moon found it lacked the necessary bulk conductivity to produce such effects. Instead, the solar wind was absorbed, merely creating a flow wake and hardly perturbing the interplanetary magnetic field (e.g. Spreiter et al., 1970; Russell et al., 1974). The moon has an electrically conducting "core", but it is so small that instead of doubling the external field as in Fig. 2(a), the perturbed surface field was enhanced by only a few percent. The moon also lacks a substantial atmosphere, and hence enough of an ionosphere to produce the alternative pressure balance obstacle. In contrast, ionospheric pressure balance currents dominated the solar wind interaction with Venus observed during the Pioneer Venus Orbiter mission, whose main features are those illustrated in Fig. 1(b). Perturbation magnetic fields associated with induced currents of either kind can exclude the external fields from the interior space of the obstacle, as suggested by both Figs. 1(b) and 2(a). Partial exclusion of the external flow and field occurs if the induced currents are insufficient or are inside the body (such as on the core) rather than on its surface. At Venus, this effect was seen as nearly field-free ionosphere beneath the ionopause when the solar wind pressure balance occurred well above the exobase at ~200 km altitude. A magnetized ionosphere was observed when the solar wind pressure exceeded the ionospheric pressure near the exobase. Under these conditions, the Venus obstacle apparently does not deflect all of the incident solar wind (Zhang et al., 1990), and the external magnetic fields diffuse into the ionosphere (e.g. Luhmann and Cravens, 1991 and references therein).

In general, an induced magnetosphere includes a wake in the form of an induced magnetotail and/or Alfven wing. As mentioned earlier in connection with Venus, the induced magnetotail is composed of inner magnetosheath flux tubes that slip over the obstacle to fill the flow wake (see Fig. 1(b)). The term Alfven wing describes the perturbations due to field-aligned currents from a conductor moving in a magnetized plasma. These currents transfer momentum between the conductor and the plasma in an effort to force them to move at the same speed. In a planetary situation field-aligned currents can also result from currents in the deflected external medium. The Alfven wing occurs when some flux tubes threading the obstacle connect to the external magnetic field. These become an effective extension of the obstacle in the external flow (see the review of satellite interactions by Kivelson, this volume). In fact, the boundaries of an induced magnetosphere are less well defined than the boundaries of the traditional magnetosphere, although it can be argued that reconnection

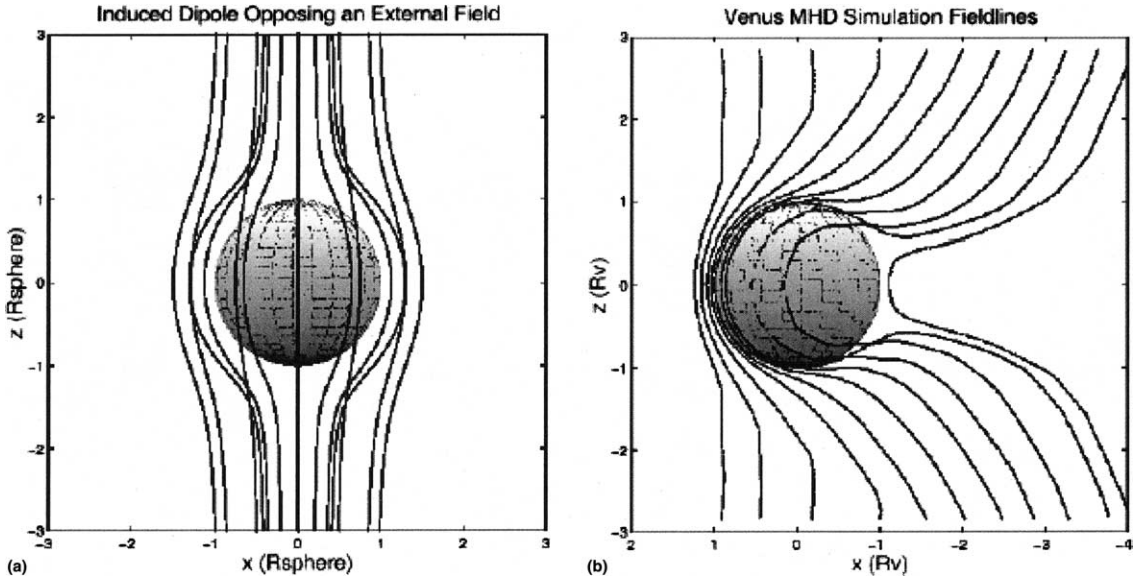

Fig. 2. (a) Illustration of the configuration of the magnetic field outside a conducting sphere, resulting from classical induction – in this case a switched on uniform external field. The perturbation field is that of an opposing dipole, which causes the external field to drape around the sphere. (b) Field line draping in a simulation of the solar wind interaction with a conducting sphere representing Venus' ionosphere, for comparison. In this case a flowing magnetized plasma encounters the obstacle boundary where magnetic field and plasma flow normal components are forced to vanish.

with the external field at the magnetopause, and ionosphere–magnetosphere coupling also compromise the traditional version. To accommodate such uncertainties, we here state our working definition of an induced magnetosphere as everything between an outer boundary outside of which the obstacle has no effect on the external medium, and an inner boundary inside of which there is no effect of the external conditions. Note that if we identified the ionopause as the inner boundary of Venus' induced magnetosphere, it would be more analogous to the inner boundary of Earth's magnetosheath, not its magnetosphere. On the other hand, the ionopause is not always impenetrable to external plasma and field, so that boundary identification even requires caution.

The adjustment of planetary ionospheres to dynamic pressure changes, and ram/wake side asymmetries, greatly complicate the separation of classical electromagnetic induction effects in induced magnetospheres. As mentioned earlier, the external magnetic field can diffuse into the ionosphere if the solar wind dynamic pressure is high (or the ionospheric pressure is weak, as at solar minimum at Venus). If magnetic fields reach the solid planet surface, conducting material in or on the body can contribute to the induced field perturbations. In the flow wake created by the external flow deflection by the obstacle, and possibly some absorption, refilling occurs due to a variety of processes. Charge separation electric fields resulting from the differing mobilities of ions and electrons in the plasma, fluid-like instabilities from the density and velocity gradients at the wake edges, and MHD and possibly even gravitational forces may all contribute. The resulting magnetic field topology of the induced magnetotail, like that of the magnetosheath, is influenced by these refilling processes as well as by mass loading by ionospheric ions as the incident flux tubes slip through the upper atmosphere. Together with the upstream deflection of the oncoming flow by the obstacle, the wakes alter the uniformity of the external magnetic field to which the conducting material of the obstacle is exposed. In addition, the conductors involved are often in unsymmetrical shapes with nonuniform conductivities. For example, a typical ionosphere is a partially conducting hemispherical shell produced on the sunlit face of the obstacle. It is moreover time variable and subject to control by forces and factors within the atmosphere (e.g. collisions, atmospheric chemistry, neutral winds, episodic production increases, and plasma pressure gradients). The isolation of the classically induced magnetic field perturbations in such settings requires careful modeling and detailed measurements. If in addition some crustal remanent magnetization is present, as at Mars (Acuña et al., 1999), all perturbation currents are affected by the distribution and strength of those permanent localized fields.

It is worth noting that the classically induced fields apparently generated at some of the Galilean satellites, and treated later in this volume by Kivelson, are not usually described in terms of induced magnetospheres. In these cases the induction is by a small oscillating equatorial component of the local Jovian magnetic field, resulting in an induced field perturbation that deflects the incident corotating plasma, but does not make the satellite an effective flow obstacle. Clearly there is some ambiguity about what qualifies as an induced magnetosphere.

Below we consider our simplest and best-observed example of an induced magnetosphere at Venus. A numerical simulation of the solar wind interaction with a conducting sphere, representing the ionosphere, reproduces the basic features observed by the Pioneer Venus magnetometer in the magnetosheath and magnetotail. We consider the possibility that under certain circumstances some time-dependent external fields leak into the interior and electromagnetically induce field perturbations in Venus' core that oppose interplanetary field changes. The signatures of this classically induced contribution, and its potential for telling us about the interior of Venus, provides some food for thought on retrospective and future studies of induced magnetospheres in the solar system.

3. Venus: the prototypical induced planetary magnetosphere

The exploration of Venus by the long-lived Pioneer Venus Orbiter (PVO) in the 70s and 80s provided a first close look at the details of the solar wind interaction with an effectively unmagnetized planet. Fig. 1(b) was essentially derived from the PVO magnetometer data and complementary plasma measurements (Russell and Vaisberg, 1983; Luhmann, 1986). The draped magnetic fields of the magnetosheath and the induced magnetotail are its key attributes. The occurrence of the primary mission of PVO during active solar conditions provided the opportunity to probe Venus' induced magnetosphere in its simplest state. Especially important in this regard were the location of the boundary where the ionospheric pressure balanced incident solar wind dynamic pressure in the practically collisionless region of the upper atmosphere, and the existence of a significant nightside ionosphere. The $\sim$10 km thick ionopause boundary layer, at $\sim$350 km altitude, carried essentially all of the current required to deflect the solar wind and shield the lower atmosphere and solid planet from the interplanetary field. Classical induction in the solid planet apparently played no significant role. To first order, Venus at solar maximum is a spherical conducting obstacle in the magnetized solar wind, with its ionospheric pressure producing the flow obstacle.

The magnetosheath of Venus was analyzed using the best tool available at the time, the Spreiter and Stahara gas-dynamic frozen-field magnetosheath model for hypersonic flow around a blunt obstacle (Luhmann et al., 1986; Phillips et al., 1986; Spreiter and Stahara, 1992). In general, the dayside fields up to the terminator plane bore remarkable resemblance to the three-dimensional magnetic field described by that model. The exception was the magnetic barrier region immediately adjacent to the ionopause, where the compressed interplanetary field plus the dynamically induced field from the ionopause currents assumed all of the incident solar wind dynamic pressure (e.g. Zhang et al., 1990). This feature is not part of the gasdynamic description because the magnetic field exerts control over the plasma here. Such domains are the counterpart of the plasma depletion layer in Earth's magnetosheath, and a key attribute of induced magnetospheres in the solar wind.

The PVO observations of the Venus wake were restricted to low (<3 Venus radii, Rv) and high altitude (10–12 Rv) segments due to the orbit sampling along the highly elliptical path of PVO. Several overviews of the PVO measurements of plasma and field structure in that region can be found in reviews by Phillips and McComas (1991), and Slavin et al. (1989). Luhmann et al. (1991), and Luhmann (1992) analyzed the PVO magnetometer observations of the low altitude wake, while Saunders and Russell (1986), and McComas et al. (1986), concentrated on its high altitude behavior in the magnetotail proper. The comet tail-like draped fields of Fig. 1(b) were clearly present in the observations, but the near-wake fields which are most affected by the induced currents "internal to" the Venus ionospheric obstacle, required more interpretation. The lack of a wake limited the applications of the gas dynamic model to the study of the Venus magnetotail (although Moore et al. (1991) made some adaptations to mimic wake closure in the gas dynamic flow, and Luhmann et al. (1991) experimented with insertion of a comet-like field structure). These limitations do not exist in recent global MHD numerical simulations, described below.

The observed near-wake of Venus exhibited two kinds of magnetic features. One was characterized by nearly antisolar field inclusions within paired low-density ionospheric regions, observed during the high solar activity primary mission (Brace et al., 1983). These features are referred to as nightside ionospheric holes due to their low densities. The details of their generation are still not understood (e.g. Luhmann and Russell, 1992), although their fields appear to be oriented toward and away from the Sun like the prevailing draped fields of the induced magnetotail. The second type of feature was large-scale magnetization, which occurred at the PVO periapsis altitudes when the incident solar wind pressure was unusually high. These cases can be interpreted as the broadening of the ionospheric layer carrying the pressure balance currents, and correspond to the dayside magnetized ionospheres (e.g. Luhmann and Cravens, 1991). From their properties Luhmann (1992) deduced that the induced magnetic fields around Venus were toroidal, consistent with near-complete wrapping of solar wind fields around the planet as in Fig. 2(b), rather than poloidal or deflected around the obstacle as in Fig. 2(a). An implication of the magnetized ionospheres is that the pressure balance currents flow in part in the collisional ionosphere, where they cause atmospheric and ionospheric modifications and may not shield the surface from the externally imposed magnetic fields (Luhmann, 1991). However, for the first global simulations of Venus' induced magnetosphere, the most ideal approximation where the ionopause carries all of the necessary currents, as on a surface, provided the best model.

Starting in the early 90s, several authors published results from the numerical MHD simulation of the solar wind interaction with a conducting sphere representing Venus' ionopause. In these simulations, the shielding currents flow where the external medium makes contact with the sphere. Simulations by Tanaka (1992, 1993) gave detailed insight on how the draped magnetic fields close on the nightside, but also drape and slip over the surface of the sphere from the poles, eventually forming the central induced magnetotail. Murawski and Steinolfson (1996) showed how the magnetic fields in the wake of the sphere could, in the presence of some diffusion, form a x-point at the anti-solar region that separated a toroidal band of low altitude field from a comet-like magnetotail structure. They found that the induced magnetotail probably requires some contribution from ionospheric mass loading of the inner magnetosheath flux tubes to produce sufficently draped fields. DeZeeuw et al. (1996) simulated a case where the external field was aligned with the flow, an untypical situation in the solar wind at Venus, but nonetheless one that is observed on occasion. Kallio et al. (1998) showed that the magnetosheath field magnitude and bow shock shape are well represented by an MHD simulation. Each study produced a picture of an induced magnetosphere that qualitatively resembles what was inferred from the PVO observations.

The magnetic field lines in Fig. 2(b) represent the global external field configuration from the particular MHD simulation described by Kallio et al. (1998). The perturbation fields are from currents both on the conducting sphere representing Venus, and in the deflected external plasma representing the solar wind. The parameters of this particular case study, carried out using methods developed for Earth magnetosphere simulations (Lyon, 2000), are: 14 nT interplanetary magnetic field (in this model perpendicular to the upstream flow direction), a magnetosonic Mach number of 4.5, and flow speed 400 km/s. The ionopause of the presumed

perfectly conducting ionosphere is represented by zero normal field and flow boundary conditions at the spherical obstacle surface. (Inclusion of an ionosphere, as in Tanaka and Murawski (1997) broadens the current carrying layer and introduces ionospheric plasma tail rays, but does not change the gross behavior of the surrounding induced magnetosphere.) The dayside fields external to the sphere in Fig. 2(b) closely resemble those draped around the classically induced dipole field (Fig. 2(a)). The most obvious exception is that the draped fields cross the terminator plane, producing a degenerate version of the induced dipole field configuration. If the cusps at the poles in Fig. 2(a) were folded back into the wake of the obstacle, one would obtain field lines similar to the simulation field geometry.

To visualize the differences between the magnetic fields generated in the simulated MHD flow interaction and the classically induced dipole case in Fig. 2(a), in Fig. 3 we subtract the background (perpendicular) solar wind field from the simulation field. As mentioned earlier, this residual field represents a combination of the field from currents on the conducting obstacle, and currents due to flow distortions of the frozen-in magnetic field. (In principle one could separately determine the field from the current on the obstacle/flow interface by computing curl of B on the sphere.) The net result is similar to the "unipolar generator" fields envisioned by Sonett and Colburn (1968), and calculated by Horning and Schubert (1974) early in the history of unmagnetized planet exploration. Although in this steady state model, there is no explicit counterpart of the classically induced currents on a conducting sphere in a time-varying field, the simulation setup for such a case study would be identical. However, the results would differ because the external field produces an asymmetric MHD interaction. At any time the magnetosheath and induced magnetotail fields would be influenced by a variety of external field orientations – as well as their associated current sheets that could give rise to reconnection sites.

The subsequent Venus induced magnetosphere simulations carried out by Tanaka and Murawski (1997)

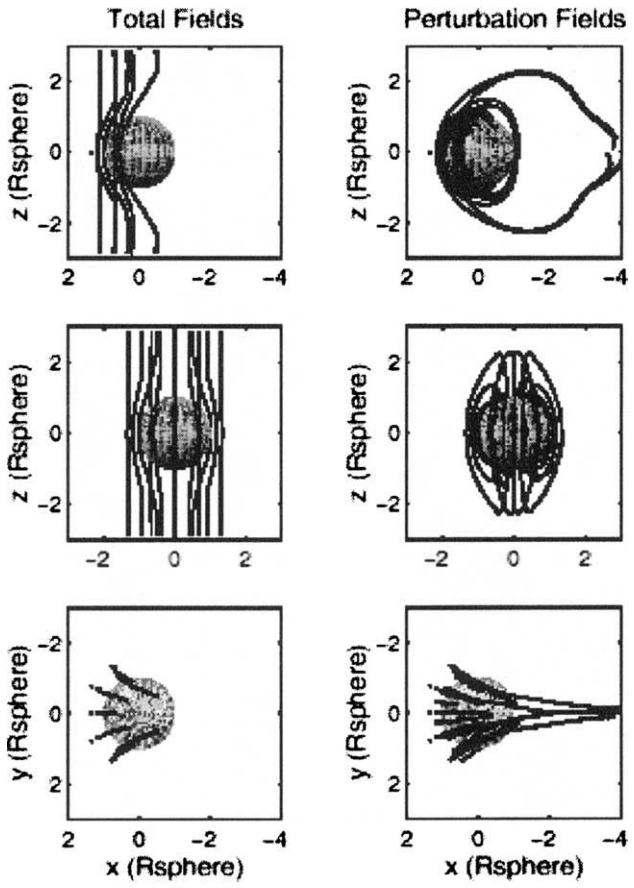

Fig. 3. 3D Projections of selected magnetic field lines from the simulation of the solar wind interaction with a conducting sphere, representing Venus (also see Fig. 2(b)). The lines are traced from the selected upstream starting points. The left panels show the full simulation field looking down on the plane of the external field (top), from the Sun (middle), and along the external field direction (bottom). The right panels show the corresponding perturbation fields in the same view, obtained by subtracting the uniform external field.

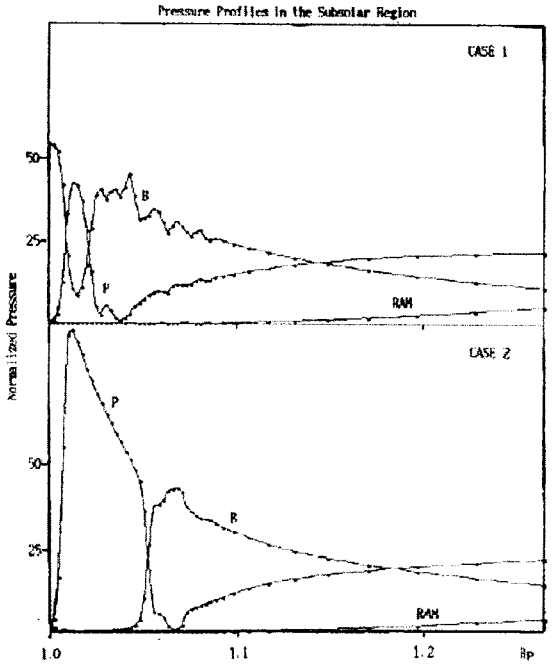

Fig. 4. Illustration from Tanaka (1993) of the gas pressure (P), magnetic pressure B2/2 (labeled B), and dynamic pressure (RAM) along the stagnation streamline of their Venus interaction simulation that included an ionosphere. The simulation does not separate the solar wind and ionospheric gas pressures, thus the shock heated solar wind makes a significant thermal pressure contribution over the radial range shown – within the magnetosheath. The lower panel represents the typical solar maximum Venus interaction where currents in the ionopause layer, at the top of the ionosphere, shield out the external flow and field. The upper panel represents periods of high dynamic pressure or low ionospheric pressure, where the interplanetary field diffuses and convects into, and possibly through, the ionosphere to the surface.

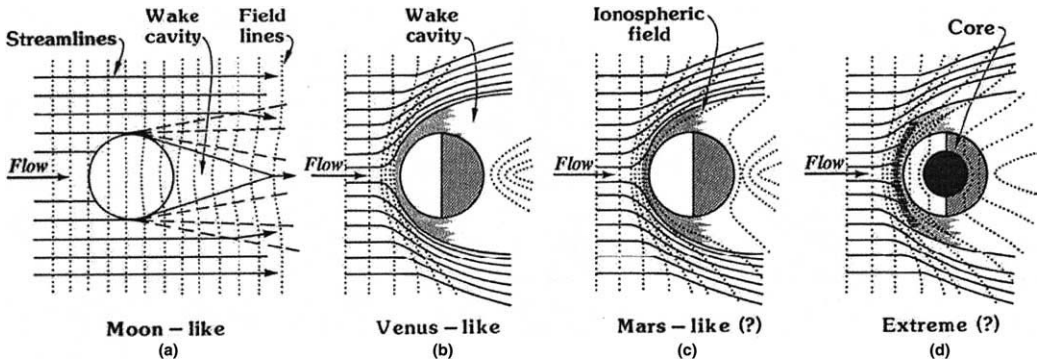

Fig. 5. Illustration of increasingly strong interactions of the solar wind with unmagnetized planetary obstacles, inferred from known objects. The Moon (a) interacts only weakly with the solar wind, providing mainly an absorber. At Venus (b), the presence of a substantial ionosphere produces a relatively impenetrable obstacle. This obstacle ceases to be impenetrable when the solar wind dynamic pressure exceeds first the ionospheric pressure at the exobase (c) (considered a common condition at Mars and at Venus at solar minimum), and finally the peak ionospheric pressure (d). The possible exposure of the solid planet to varying interplanetary fields may produce a classical induction signature near Venus' surface. The scenario in panel (d) has not been subjected to observational testing.

that included the ionospheric plasma provided more insight into the variety that the real solar wind interaction exhibits. These simulations reproduced the magnetization of the ionosphere that was observed to occur on PVO when incident solar wind magnetic pressure pushed the ionopause downward (e.g. see Luhmann and Cravens, 1991). The associated altitude profiles of the simulated pressure along the stagnation streamline, showing the trade-off from solar wind dynamic pressure to magnetic barrier pressure to ionospheric pressure are reproduced in Fig. 4. The magnetic field extends to the surface in the high solar wind dynamic pressure case (top panel), raising the question of what happens on Venus on such occasions. While the lowest altitude field structure is probably not spatially resolved in the simulation shown, calculations by Luhmann (1991), based on the PVO periapsis field measurements, indicate that some field is probably present at the surface on occasion. Perhaps, as mentioned earlier and suggested by the sequence of sequentially stronger interaction concepts in Fig. 5, classical induction in the core of Venus produces an additional magnetic field perturbation. In theory, this perturbation could be measured on the surface to gain information about Venus' core, if it could be separated from the surface fields due to currents in the ionosphere and above. Of course this illustration presumes there are no additional good conductors on the Venus surface or in the crust and mantle.

4. Concluding remarks

While the idea of an induced magnetosphere at first seems straightforward, the discussion here suggests it is not a particularly well-constrained concept when applied to even the simplest solar system cases, as at Venus. At Venus we are at least fortunate to have a substantial observational picture of what appears to first-order the interaction of the solar wind with a conducting sphere. Global MHD simulations suggest how the combination of ionopause boundary currents, and distributed currents from the external plasma flow deflection, lead to the field perturbations that characterize Venus' induced magnetosphere. Yet we have only scratched the surface of even this simplest planetary example. Observations within the Venus ionosphere, and on its surface, under a range of solar wind and ionospheric conditions, would be necessary to truly characterize the breadth of characteristics of Venus' induced magnetosphere. Perhaps more easily, the numerical simulations could be further exploited to explore the numerous possible scenarios of the Venus solar wind interaction that must occur.

The Venus induced magnetosphere will be revisited with modern instruments by Venus Express, planned for launch in 2005. The induced magnetospheres at Mars and Titan, which are further complicated by strong crustal remanent fields (e.g. Liu et al., 1999) and finite ion gyroradius effects (Brecht et al., 2000; Ledvina et al., this volume), respectively, are the new frontier. Observations from the Mars Express mission starting in 2004 are expected to shed light on the Mars-solar wind interaction, while the Cassini Orbiter will repeatedly fly by Titan with a full complement of particles and fields instruments. Broadly viewing induced magnetospheres in terms of their systems of classically and dynamically induced currents resulting from their magnetized plasma interactions, one could also study these cases in some detail by using numerical simulations to experiment with possible scenarios (e.g. as done by Ledvina et al., this volume, for Titan in the solar wind). Indeed, the combination of observations and simulations is required to explore the physical complexity and variety of plasma interactions that induced magnetospheres encompass.

Acknowledgements

This report was written under support from the Cassini Ion Neutral Mass Spectrometer Investigation, via a subcontract from NASA through the University of Michigan-Award F006454. We thank John Lyon for providing the results of his MHD simulation of the Venus-solar wind interaction for our use.

References

Acuña, M.H., Connerney, J.E.P., Ness, N.F., et al. Global distribution of crustal magnetism discovered by the Mars Global Surveyor MAG/ER Experiment. Science 284, 790–793, 1999.

Bagenal, F., Cravens, T.E., Luhmann, J.G., McNutt, R.L., Cheng, A.F. Pluto's interaction with the solar wind, in: Vilas, F. (Ed.), Pluto. University of Arizona Press, Tucson, pp. 523–555, 1998.

Brace, L.H., Taylor Jr., H.A., Gombosi, T.I., Kliore, A.J., Knudsen, W.C., Nagy, A.F. The ionosphere of Venus: observations and their interpretation, in: Hunten, D., Colin, L., Donahue, T., Moroz, V. (Eds.), Venus. University of Arizona Press, Tucson, pp. 779–840, 1983.

Brecht, S.H., Larson, D.J., Luhmann, J.G. Simulation of the Saturnian magnetospheric interaction with Titan. J. Geophys. Res. 105, 13,119–13,130, 2000.

DeZeeuw, D.L., Nagy, A.F., Gombosi, T.I., Powell, K.G., Luhmann, J.G. A new axisymmetric MHD model of the interaction of the solar wind with Venus. J. Geophys. Res. 101, 4547–4556, 1996.

Horning, B.L., Schubert, G. Steady state asymmetric planetary electrical induction. J. Geophys. Res. 79, 5077–5088, 1974.

Kallio, E., Luhmann, J.G., Lyon, J.G. Magnetic field near Venus: a comparison between Pioneer Venus Orbiter magnetic field observations and an MHD simulation. J. Geophys. Res. 103, 4723–4737, 1998.

Lindgren, C.J., Cravens, T.E., Ledvina, S.A. Magnetohydrodynamic processes in the inner coma of comet Halley. J. Geophys. Res. 102, 17,395–17,406, 1997.

Liu, Y., Nagy, A.F., Groth, C., DeZeeuw, D., Gombosi, T., Powell, K. 3D multifluid MHD studies of the solar wind interaction with Mars. Geophys. Res. Lett. 26, 2689–2692, 1999.

Luhmann, J.G. Induced magnetic fields at the surface of Venus inferred from Pioneer Venus Orbiter near-periapsis measurements. J. Geophys. Res. 96, 18,831–18,840, 1991.

Luhmann, J.G. The solar wind interaction with Venus. Space Sci. Rev. 44, 241–306, 1986.

Luhmann, J.G. Pervasive large-scale magnetic fields in the Venus nightside ionosphere and their implications. J. Geophys. Res. 97, 6103–6121, 1992.

Luhmann, J.G., Cravens, T.E. Magnetic fields in the ionosphere of Venus. Space Sci. Rev. 55, 201–274, 1991.

Luhmann, J.G., Russell, D.S. Magnetic fields in Venus nightside ionospheric holes: collected Pioneer Venus Orbiter magnetometer observations. J. Geophys. Res. 97, 10267–10282, 1992.

Luhmann, J.G., Russell, C.T., Schwingenschuh, K., Yeroshenko, Y. A comparison of induced magnetotails of planetary bodies: Venus, Mars and Titan. J. Geophys. Res. 96, 11,199–11,208, 1991.

Luhmann, J.G., Warniers, R.J., Russell, C.T., Spreiter, J.R., Stahara, S.S. A gas dynamic magnetosheath field model for unsteady interplanetary fields. Application to the solar wind interaction with Venus. J. Geophys. Res. 91, 3001–3010, 1986.

Lyon, J.G. The solar wind–magnetosphere–ionosphere system. Science 288, 1987–1991, 2000.

McComas, D.J., Spence, H.E., Russell, C.T., Saunders, M.A. The average magnetic field draping and consistent plasma properties of the Venus magnetotail. J. Geophys. Res. 91, 7939–7953, 1986.

Moore, K.L., McComas, D.J., Russell, C.T., Stahara, S.S., Spreiter, J.R. Gas dynamic modeling of the Venus magnetotail. J. Geophys. Res. 96, 5667–5681, 1991.

Murawski, K., Steinolfson, R.S. Numerical modeling of the solar wind interaction with Venus. Planet. Space Sci. 44, 243–252, 1996.

Ness, N.F., Acuna, M.H., Behannon, K.W., Neubauer, F.M. The induced magnetosphere of Titan. J. Geophys. Res. 87, 1369–1381, 1982.

Phillips, J.L., McComas, D.J. The magnetosheath and magnetotail of Venus. Space Sci. Rev. 55, 1–80, 1991.

Phillips, J.L., Luhmann, J.G., Russell, C.T. The magnetic configuration of the Venus magnetosheath. J. Geophys. Res. 91, 7931–7938, 1986.

Russell, C.T., Vaisberg, O. The interaction of the solar wind with Venus, in: Hunten, D., Colin, L., Donahue, T., Moroz, V. (Eds.), Venus. University of Arizona Press, Tucson, pp. 873–940, 1983.

Russell, C.T., Coleman, P.J., Lichtenstein, B.R. The permanent and induced magnetic dipole of the moon, in: Proceedings of the Fifth Lunar Conference, vol. 3, pp. 2747–2760, 1974.

Saunders, M.A., Russell, C.T. Average dimension and magnetic structure of the distant Venus magnetotail. J. Geophys. Res. 91, 5589–5604, 1986.

Slavin, J.A., Intriligator, D.S., Smith, E.J. Pioneer Venus orbiter magnetic field and plasma observations in the Venus magnetotail. J. Geophys. Res. 94, 2383–2398, 1989.

Sonett, C.P., Colburn, D.S. The principle of solar wind induced planetary dynamos. Phys. Earth Planet. Interiors 1, 326–346, 1968.

Spreiter, J.R., Stahara, S.S. Computer modeling of solar wind interaction with Venus and Mars. Venus and Mars: Atmospheres, Ionospheres, and Solar Wind Interactions. AGU Monograph 66. American Geophysical Union, Washington, DC, pp. 345–385, 1992.

Spreiter, J.R., Marsh, M.C., Summers, A.L. Hydromagnetic aspects of solar wind flow past the moon. Cosmic Electrodyn. 1, 5–50, 1970.

Tanaka, T. Three dimensional magnetohydrodynamic simulation of the unstructured system using the finite element TVD scheme. Comput. Fluid Dyn. 1, 14–26, 1992.

Tanaka, T. Configurations of the solar wind flow and magnetic field around the planets with no magnetic field: calculation by a new MHD simulation scheme. J. Geophys. Res. 98, 17,251–17,262, 1993.

Tanaka, T., Murawski, K. Three-dimensional MHD simulation of the solar wind interaction with the ionosphere of Venus: results of two-component reacting plasma simulation. J. Geophys. Res. 102, 19,805–19,821, 1997.

Zhang, T.L., Luhmann, J.G., Russell, C.T. The solar cycle dependence of the location and shape of the Venus bow shock. J. Geophys. Res. 95, 14,961–14,967, 1990.